Marine Geodesy, 27: 31–45, 2004

ISSN: 0149-0419 print / 1521-060X online
DOI: 10.1080/01490410490465274

Taylor & Francis
Taylor & Francis Group

TOPEX/Poseidon and Jason Equatorial Sea Surface Slope Anomaly in the Atlantic in 2002: Comparison with Wind and Current Measurements at 23W

C. PROVOST
S. ARNAULT
N. CHOUAIB
A. KARTAVTSEFF
L. BUNGE
E. SULTAN

LODYC UMR7617 CNRS/IRD/UPMC/MNHN
Université Pierre et Marie Curie
Paris, France

A time series of velocity profile in the upper 150 m of the equatorial Atlantic was gathered at 23W in 2002 within the PIRATA program. It constitutes the first time series of near surface current measurements simultaneous with altimetric data in the equatorial Atlantic. The surface slope anomaly along the equator is computed from satellite altimetry, and, as a proxy for the pressure gradient along the equator, compared with the wind and near surface current data. In a first step, a time series of the surface slope anomaly along the equator in the Atlantic is computed from the 10-year-long TOPEX/Poseidon sea level anomalies. A sensitivity study establishes the robustness of the calculation. Apart from a 15 cm bias, the equatorial sea surface slope anomalies estimated either from TOPEX/Poseidon or from Jason over the 6-month overlap (Feb.–Aug. 2002) do not reveal drastic differences. We produce two sea surface slope anomaly composite time series for 2002 (one with T/P data, the other with Jason data during the commissioning phase) and compare them to the wind and velocity data at 23W. As expected, the near surface velocity and depth of the upper limit of the equatorial undercurrent (EUC) are extremely well correlated with the surface pressure gradient anomaly. 10-year-long time series of altimetry-derived zonal sea surface slope anomaly and ECMWF ERA40 wind stress are also well correlated. They exhibit similar spectral content and similar anomalous years. This is a first step towards a full analysis of the EUC dynamics using altimetry, PIRATA data (near surface current and subsurface thermohaline structure) and model. These initial comparisons reinforce the utility of Jason measurements for continuing the 10-year and highly accurate TOPEX/Poseidon time series for study of equatorial signals.

Keywords satellite altimetry, equatorial dynamics, Atlantic ocean, sea surface slope, wind, equatorial currents

Received 19 December 2002; accepted 28 January 2002.

This research was funded by the French Ministry of Research (ACI Climat), the IRD (Institut de Recherche pour le Développement) and CNES (Centre National de Recherche Spatiale) institutions. We thank Joël Sudre, Joël Dorandeu, and Yves Ménard for their advice about altimetric data and PIRATA chairmen J. Servain, J. Lorenzzetti and M. McPhaden. We deeply acknowledge the help of the Lanoisellé family and crew members from *Atalante* and *Le Suroit* for mooring construction deployment and recovery.

Address correspondence to C. Provost, LODYC UMR7617 CNRS/IRD/UPMC/MNHN, Université Pierre et Marie Curie, 4 place Jussieu, Tour 45-5ème étage, Case 100, 75252, Paris, Cedex 05 75252, France. E-mail: cp@lodyc.jussieu.fr

During last decades, satellite altimetry has proven a powerful means of acquiring synoptic scale data for a variety of ocean surface phenomena. SEASAT, GEOSAT, ERS, and TOPEX/Poseidon have provided highly accurate measurements of sea surface height (SSH) and have contributed significantly to many topics of oceanography and geodesy (Fu and Cazenave 2001). In the tropical Atlantic, satellite altimetric data have been used to examine seasonal and interannual variations (e.g., Arnault and Cheney 1994; Arnault and Kestenare 2004; Arnault et al. 2004; Ménard 1988). However, few attempts of purely equatorial 2N-2S dynamics (vanishing of the Coriolis force) study have yet been realized.

In the Atlantic, the equatorial thermocline, region of very high thermal gradients that separates the warm surface water from colder water at depth, has a depth of about 150 m in the west and its surfaces in the east. This slope implies an eastward pressure force in the upper ocean. Thus, surfaces of constant pressure, including the sea surface slope downward from west to east. This zonal slope and the associated eastward pressure force cannot be balanced by Coriolis force at the equator and a swift jet is observed flowing down-gradient in the thermocline: the equatorial undercurrent (EUC). This strong jet flows eastward, against the prevailing trade winds, with speeds that can reach 1.5 m/s. It has its core in the thermocline and extends vertically over a depth of 150 m. Although its width is of the order of 200 km, the current is continuous over a longitudinal distance of more than 4000 km in the Atlantic. It is hidden from direct view by a surface current normally flowing westward. As the equatorial thermocline slopes upward to the east, the EUC, embedded in the thermocline, flows upward with the isopycnals.

Ocean currents and temperature fields near the equator adjust to wind stress variations on monthly time scales, primarily through the excitation of equatorial baroclinic Kelvin and long Rossby waves. The tropical Atlantic is dominated by a strong annual cycle forced by the seasonally varying trade winds. The zonal slope of the thermocline varies practically in phase with the winds in the tropical Atlantic (Katz et al. 1986). The thermocline is relatively horizontal during the first half of the year when the winds along the equator are weak, and it has a steep slope when the westward winds are intense during the second half of the year.

Altimetry at the equator in the Atlantic has not yet been used to examine the slope at the surface and relate it to the surface and subsurface structures, mainly because of the lack of simultaneous in situ time series. The PIRATA (PIlot Research Array moored in the Tropical Atlantic) project for meteorological and upper ocean measurements maintains a network of surface or near-surface measurements with the principal objective of describing and understanding the evolution of sea surface temperature (SST), upper ocean thermal structure, and air-sea fluxes of momentum, heat, and fresh water in the tropical Atlantic on seasonal to interannual time scales. In 2002 the PIRATA array comprised an equatorial mooring measuring near surface ocean velocities. The first near surface current time series gathered during the satellite altimetry era was thus obtained in 2002. Year 2002 corresponds to the switch from TOPEX/Poseidon to JASON with a period of six months during which the two satellites were flying on the same tracks with a few minutes delay. In this article we compute the zonal sea surface slope anomaly at the equator, examine the robustness of the calculation, and compare altimetry-derived sea surface slope anomaly to in situ data. The 6-month overlap period is used to carefully compare TOPEX/Poseidon and Jason derived sea surface slope anomalies.

The next section describes the data and data processing. Then results are presented in terms of satellite/in situ comparisons. Discussion, conclusion, and perspective follow.

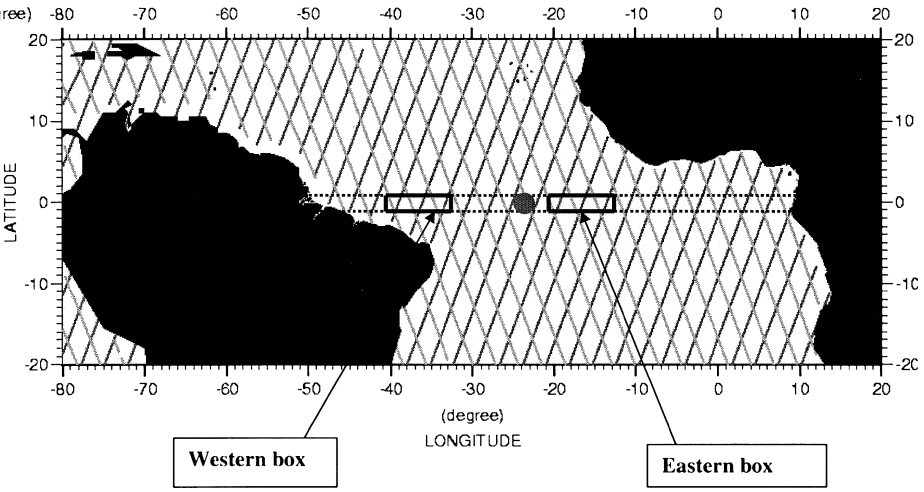

FIGURE 1 T/P and Jason tracks over the tropical Atlantic. The PIRATA current meter mooring (red dot) is located at 23W and the equator. The western and eastern boxes are straddling the equator with 2° latitudinal extension. Sensitivity of the time evolution of their mean value to their longitudinal extension and their center location on the equator is examined (see text). The sea level slope anomaly time series is computed as the time series difference between the mean value over the western and eastern boxes divided by the distance between box centers.

Data Processing

TOPEX/Poseidon Altimetric Data

TOPEX/Poseidon (hereafter T/P) geophysical data records (GDR) were processed over the Atlantic Ocean (Figure 1). Standard corrections for the troposphere (wet tropospheric correction from on-board radiometer), ionosphere (TOPEX dual frequency measurements), sea state bias (Ku band, BM4 formulation), inverse barometer (referenced to a constant mean pressure), earth and pole tides were applied. We used the last version of the Texas University tide model for tidal corrections. Erroneous data with Sea Level Anomalies (hereafter SLA) greater than 100 cm were discarded from the analysis and final filter (50 km) was operated along track to remove small scale disturbances. The T/P SLA were then averaged over a 2° longitude and 2° latitude grid straddling the equator. The resulting time evolution of SLA along the equator from November 1992 to August 2002 is shown on Figure 2. The signal is very noisy to the west of 42W: this is the region of the North Brazil Current dominated by an energetic mesoscale field which is not relevant for our purpose of examining zonal pressure gradient. Except for this part, the signal at the equator presents coherent large scale structures and exhibits a strong seasonal signal, modulated by some interannual variability. To estimate the zonal slope anomaly, we averaged the SLA values over longitudinal ranges representative of the eastern and western part of the basin and computed the difference (western and eastern boxes of Figure 1). Such an example is shown on Figure 3, where the boxes are 10 degrees wide and centered, respectively, on 40W (western box) and 15W (eastern box). We performed sensitivity studies by varying the width and mean location of the western and eastern boxes. As an example, the time series difference between the mean SLA of two boxes centered on 35W (representative of the western SLA), one being 10 degree longitude wide and the other 14, has a mean of 3.2 mm and a standard deviation

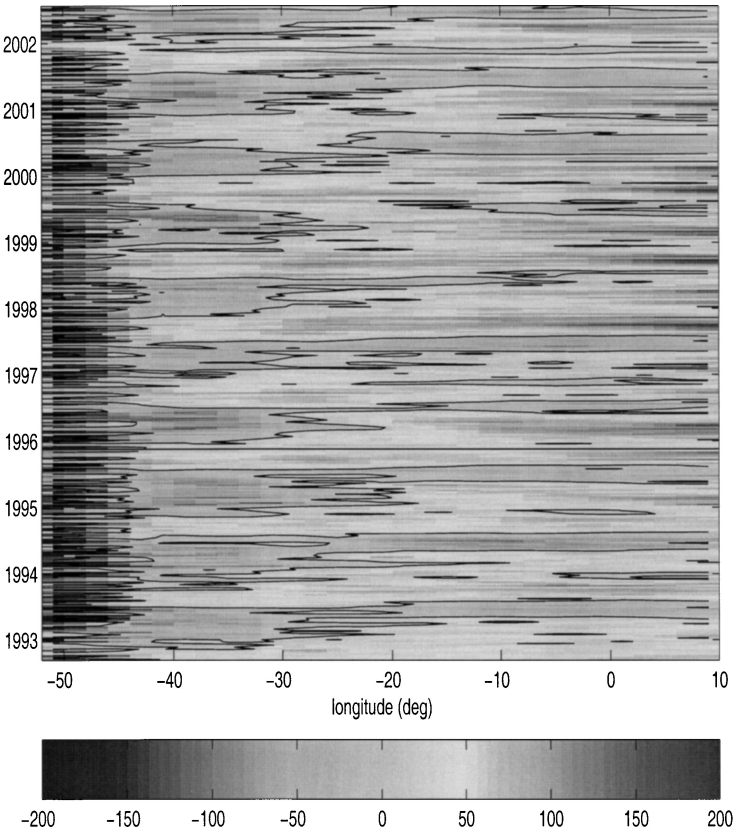

FIGURE 2 Time longitude plot of the SLA along the equatorial rail (1°N–1°S). Except for the high frequencies to the west of 42W which correspond to the mesoscale activity in the North Brazil Current, the SLA exhibits large scale patterns dominated by an annual cycle with significant interannual variability. Scale unit: mm

of 3.3 mm (Figure 4). Other sensitivity studies shown in the result section demonstrate that the error bar on the sea surface slope anomaly (SSSA) is less than 1 mm/degree whereas the annual signal has an amplitude of about 10 mm/degree.

Jason Altimetric Data

The Jason GDRs were processed in a similar way. Standard corrections were applied: troposphere (wet tropospheric correction from on-board radiometer), ionosphere (Jason dual-frequency measurements), sea state bias, inverse barometer (referenced to the time varying mean pressure of the global surface atmospheric pressure over the oceans), and earth and pole tides. (For more details, see the AVISO and PODAAC User Handbook IGRD, and GDR JASON Products, SMM-MU-M5-OP-13184-CN (AVISO), JPL D-21352 (PODAAC), Ed. 1.0, 2001.) We used the FES99 tide model for tide corrections. Jason SLAs are computed with reference to a T/P derived mean sea level. During about six months, Jason and T/P satellites were flying on the same tracks with a few minutes time lag. During that period (18 cycles), the mean bias over all tracks in the region (20N–20S) is 150 mm. Although it does not make any difference for the sea slope anomaly computation, this bias is subtracted from the Jason SLA for sake of homogeneity. The zonal slope anomaly at the

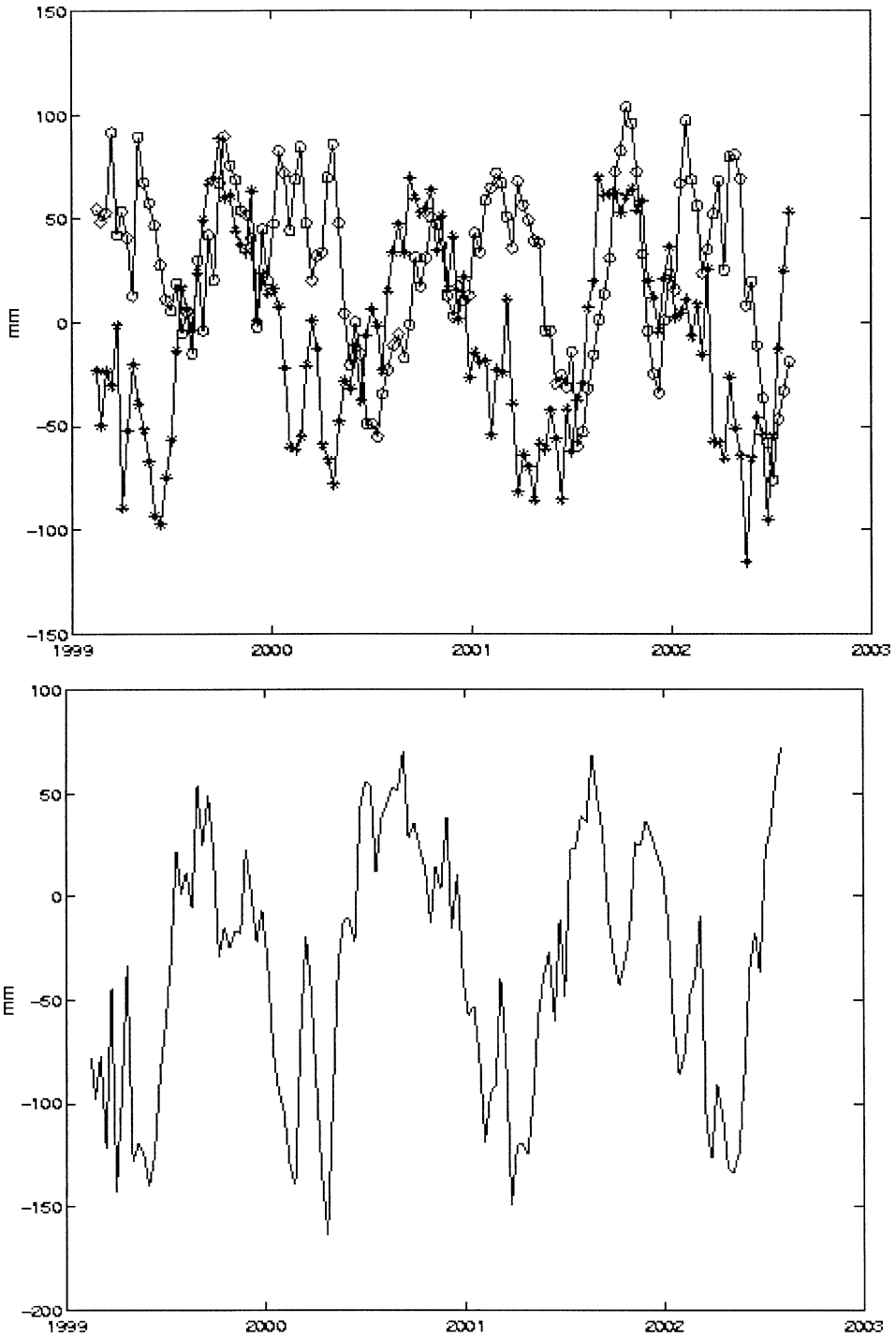

FIGURE 3 (a) SLAs in the equatorial rail (1°N–1°S): crosses for mean values in the box limited by 45 and 35W, circles for values between 20 and 10W (units: mm). (b) Difference of the above mean values divided by the distance between the centers (respectively at 40W and 15W) of the boxes (units: mm/degree).

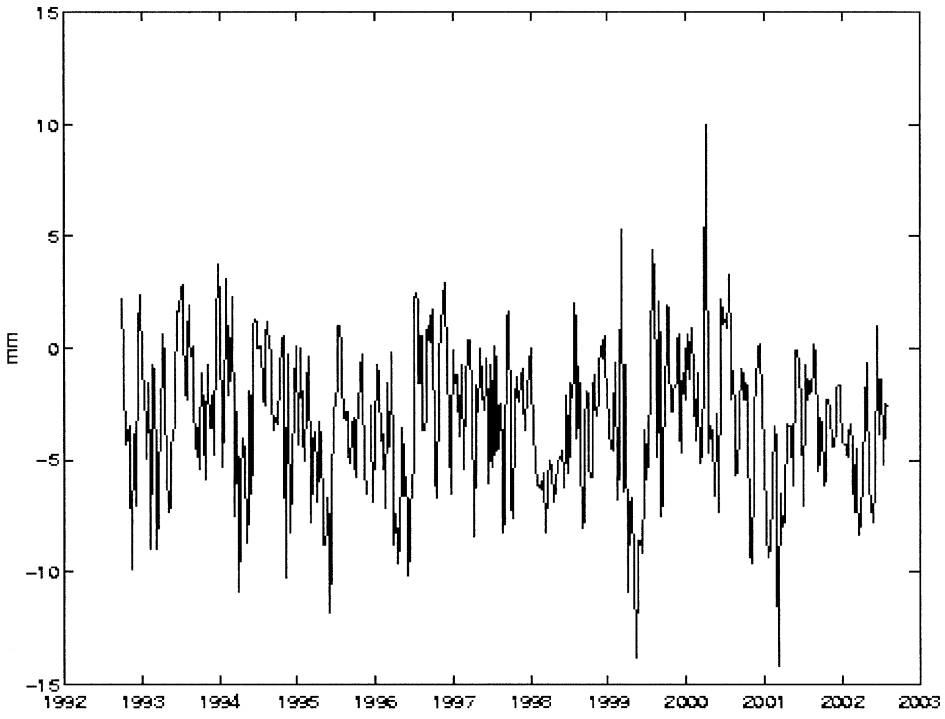

FIGURE 4 Sensitivity of the western SLA mean to the size of the box. The time series difference between the mean SLA of two boxes centered on 35W, one being 10 degree longitude wide and the other 14, has a mean of 3.2 mm and a standard deviation of 3.3 mm (units: mm).

equator is obtained in a similar way as was done for T/P data. Sensitivity studies of the choice of the western and eastern boxes provide similar error bars (see result section).

PIRATA Current Profile Data

PIRATA is an international program (France, Brazil, USA) (http://www.brest.ird.fr/pirata/pirataus.html). The purpose of PIRATA is to study ocean-atmosphere interactions in the tropical Atlantic that are relevant to regional climate variability on seasonal, interannual, and longer time scales. A mooring located at the equator and 23W was designed to monitor advection of surface water and its role in sea surface temperature changes. The first PIRATA current meter mooring was deployed in December 2001 from *RV Atalante* and recovered in December 2002 from RV Le Suroit. The near surface current meter was a Workhorse Sentinel Acoustic Doppler Current Profiler (ADCP 300 KHz). The data processing is detailed in Kartavtseff and Provost (2003). The ADCP was located at 130 m depth (between 126.5 and 154.1 m) and provides profiles of the horizontal components of the velocity between 130 m and 12 m with a vertical resolution of 4 m and a time step of one hour. Daily averages were performed. Figure 5 shows the time evolution (daily resolution) of the zonal and meridional winds at 10 m from the PIRATA buoy next to the ADCP mooring and the time depth contour of the zonal and meridional velocities.

The minimum of the magnitude of both local wind components in April corresponds to a shallower location of the EUC (core is at 60 m, upper part of the EUC less than 10 m from the surface) and intensifying of the EUC core (max zonal velocity in excess of 1 m/s).

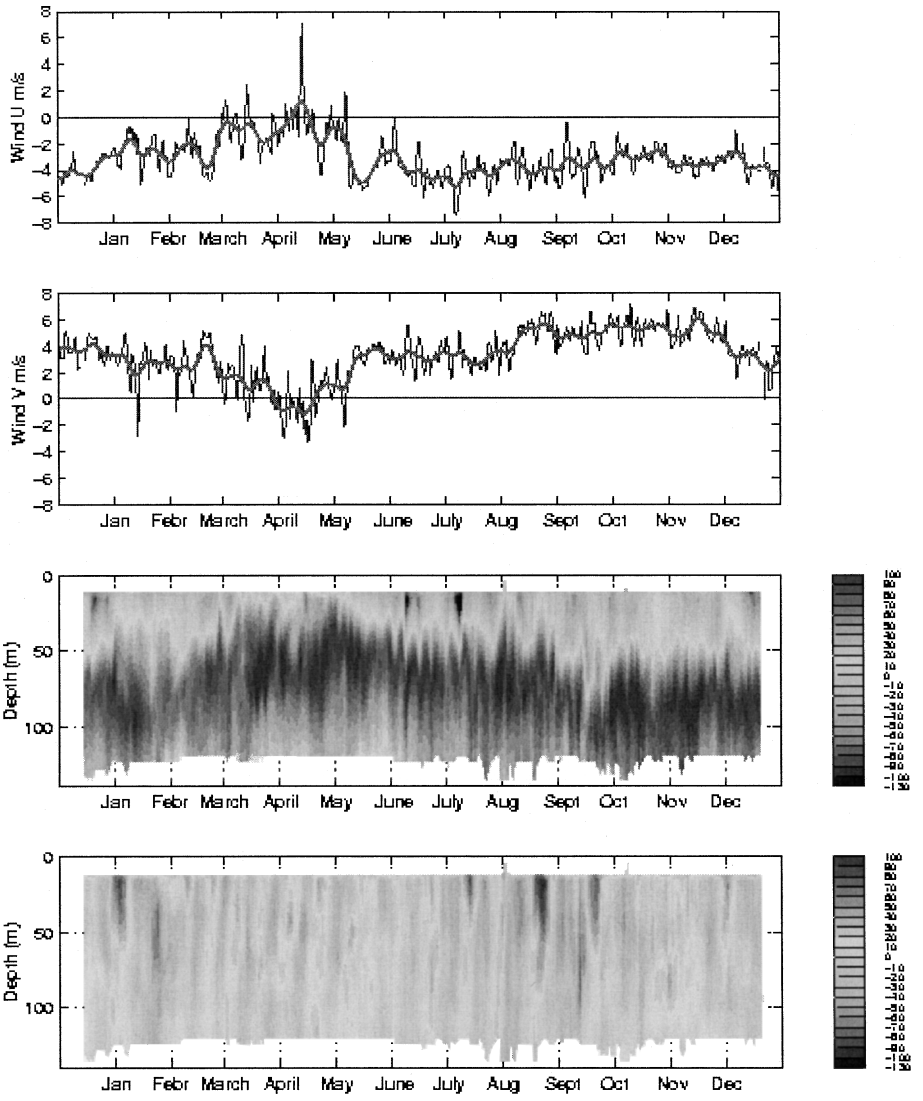

FIGURE 5 (Upper) Wind at the Pirata buoy at 23W and the equator in 2002; in blue, daily values, in red, 10-day running mean. Zonal (U) and meridional (V) components in m/s. The trade winds relax to zero in April. Tickmarks for the first day of each month. (Middle) Depth time plot of the zonal velocity (units: m/s). The EUC (red) exhibits velocities as high as 1 m/s, and its core fluctuates between 100 and 50 m depth. Velocities at 12 m reach peaks of 1.3 m/s in July (westward) and are eastward (0.2 m/s) in March–April. Eastward surface flow also occurs during Tropical Instability Wave events which start in June and persist throughout the second half of the year. (Lower) Depth-time plot of the meridional velocity (units: m/s): Oscillations extend coherently in the vertical. Peak velocities of 0.9 m/s are observed in both directions (north and south).

The magnitude of both local wind components increases at the beginning of May. Almost immediately, the westward surface flow intensifies and the EUC core deepens to reach 100 m in mid-September. After a brief intermediate state where the EUC core velocity weakens, it intensifies again but ends up only slightly faster in the fall than in the spring. The June

to December period of strong winds also corresponds to a deepening of the thermocline. High frequency fluctuations at 20–30-day periods are present throughout the year. They correspond to tropical instability waves (TIW) (Weisberg and Weingartner 1988) and are particularly visible in the meridional velocities where they vary coherently throughout the upper 130 m of the water column. A full oceanographic description and interpretation of this nice time series is not the purpose here.

For our comparison with the SSSA, we extracted the following parameters: zonal velocity at different levels, depth of the first zero of the zonal velocity (i.e., upper vertical boundary of the EUC), depth of the EUC core (i.e., depth of the maximum velocity in the EUC), and the mean zonal velocity over the EUC. These parameters were then averaged over 10 days in order to obtain the same temporal resolution as the altimetric data.

Wind Data

We use two sources of wind data: the direct wind speed components measured by the PIRATA buoy at 23W (Figure 5 upper panels) and the wind stress (Nm^{-2}) obtained from the European Centre for Medium Range Weather Forecasting (ECMWF) reanalyses (ERA 40). The new reanalysis ERA-40 covers the period from mid-1957 to 2001, including the earlier ECMWF reanalysis ERA-15, 1979–1993. The three dimensional variational technique is applied to produce the analyses every six hours. Analysis involves comprehensive use of satellite and in situ data (including the PIRATA wind data). We simply computed the wind stress at 23W and the equator by averaging the values at the four ECMWF grid points around 23W (22.5W 0.5N; 22.5W 0.5S; 23.5W 0.5N and 23.5W 0.5S) and filtering using a running mean average to produce a time series at the T/P and Jason times (every 9.91 days, precisely).

Results

Comparisons Between T/P and Jason

An example of sensitivity study of the SSSA to the choice of the western and eastern boxes is shown on Figure 6. Five cases are shown with T/P and five with Jason. In all cases, the western box on which the western mean value is computed is 40W 34W. The eastern box is variable: its width varies between 25 and 10 degrees and its center between 12.5 and 20W. For each satellite, the different slope estimates agree within 1 mm/degree. Jason and T/P estimates agree within 1.5 mm/degree except for Jason cycles 10, 11, and 12 (respectively T/P cycles 353, 354, and 355, i.e., April–May 2002). For those three successive cycles the difference between Jason and T/P is on the order of 3 to 4 mm/degree. AVISO validation reports indicate that quite a number of T/P tracks are missing over the Tropical Atlantic for cycle 353, DORIS orbit is not so good as is usual (3.21 cm r.m.s. instead of about 2 cm), and the difference between TOPEX and DORIS ionospheric correction is about 50% larger than usual (3.3 cm for ascending tracks instead of 2.3). On the other hand, nothing similar could be found for T/P cycles 354 and 355. Maps of T/P-Jason SLA differences as given in Jason-1 GDR Quality Assessment Reports (e.g., Jason-1 GDR Quality Assessment Report cycle 11 24-04-2002 04-05-2002 SALP-RP-P2-EX- 21072-CLS011) reveal some important differences along the equator in the Gulf of Guinea during that period. They could be linked to a combined effect of orbit and sea state bias (based on sea wave height measurements) errors. Indeed, precise sea state bias determination is still needed for Jason GDR. However our results are encouraging concerning the use of Jason data to complete T/P ones in terms of equatorial sea surface slope variability.

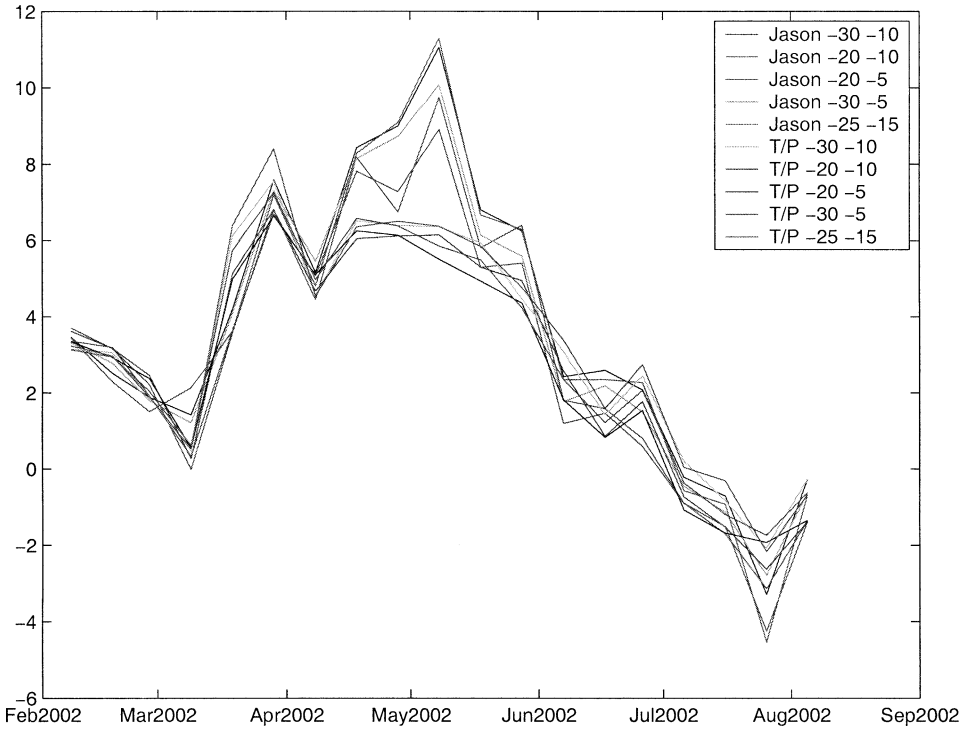

FIGURE 6 Comparison of the equatorial slope anomaly for T/P and Jason in mm/degree over the commissioning phase. The western box is 40W 34W; the eastern box is variable both in location and size: 20W 5W, 20W 10W, 30W 10W, 25W 15W, 30W 5W. Sensitivity to the choice of the box is less than 1 mm/degree. Sea surface slope anomalies from Jason GDR are within 2mm/degree of those derived from T/P except for cycles 10, 11, and 12 (greater by up to 6 mm/degree).

Comparison Between 10-Year-Long Time Series of Altimetry-Derived Sea Surface Slope Anomaly and Wind Stress from ERA40

The SSSA computed from 10 years of T/P is shown on Figure 7a. From the robustness of the previous results regarding the box choices, we use 34W 40W as western box limits and 30W 10W for the eastern one. The SSSA exhibits a strong seasonal cycle with an amplitude of about 10 mm/degree on average, a minimum usually in August–September and a maximum in May–June. Although the seasonal cycle is dominant, interannual variability is important both in amplitude and in phase. For example, variations in slope anomaly in 1997 are small. The singularity of year 1997 has also been observed in terms of surface geostrophic currents derived from T/P over the whole Tropical Atlantic (Arnault and Kestenare 2004). To date no explanation for this oceanic circulation anomaly has been found. Besides the 12-month period, a spectrum analysis of the 10-year-long equatorial SSSA time series reveals some energy at six months and at three years.

A rapid analysis shows that the ERA40 wind stress amplitude (Figure 7b) is extremely well correlated with the SSSA (correlation of 0.67 with the wind leading the SSSA by about 10 days). The wind stress exhibits a spectral content similar to the slope anomaly, a huge seasonal cycle, some energy at six months and at three years. Year 1997 is also a singular year in the wind stress time series at 23W with weak values. Although interesting to remark, this 1997 anomaly is beyond the scope of this study, which deals with 2002 data sets.

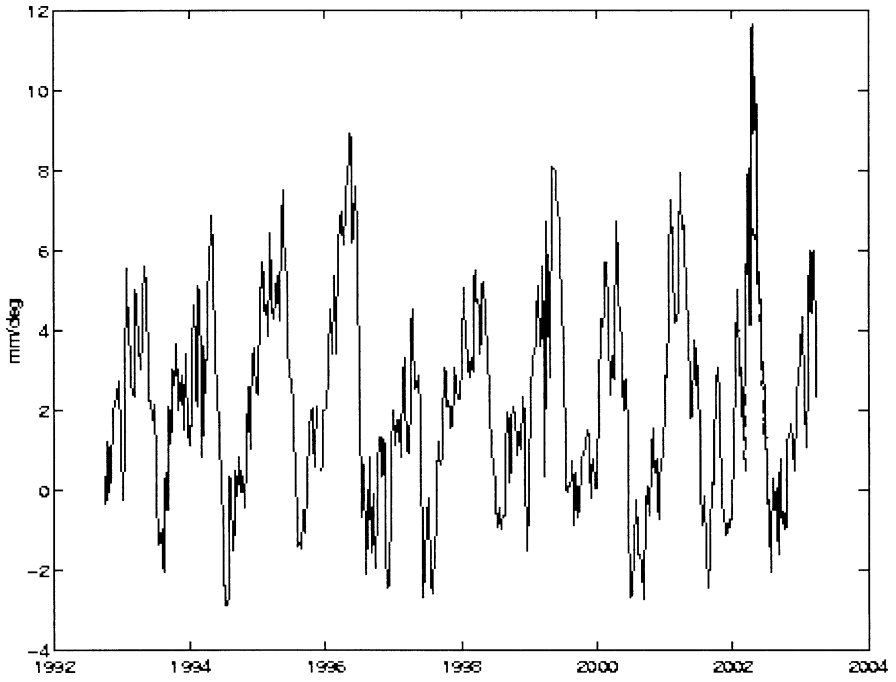

(a)

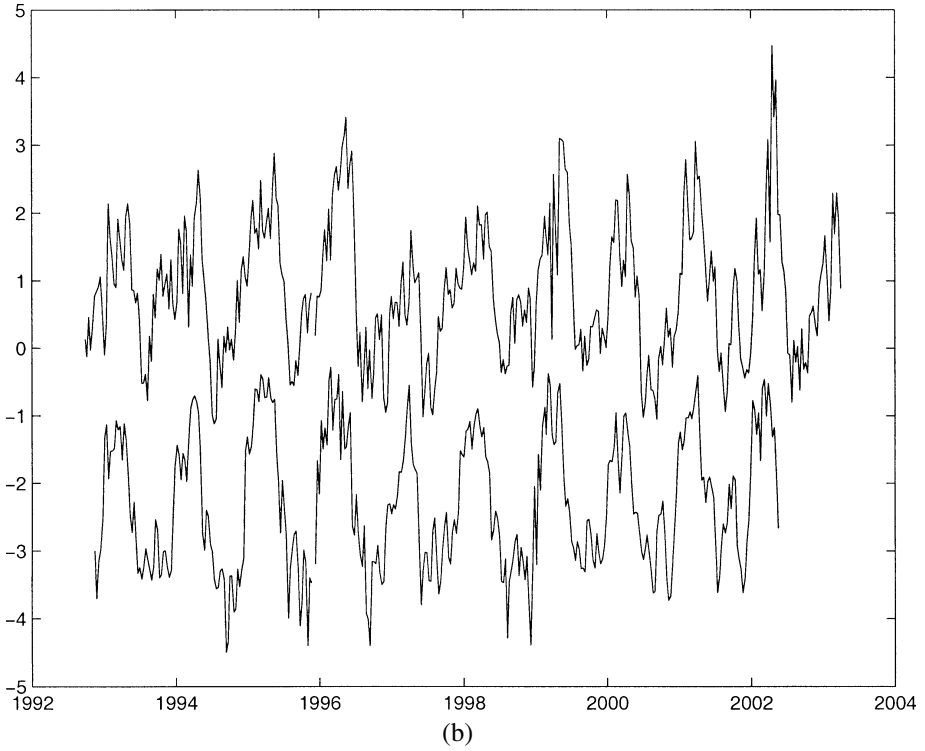

(b)

FIGURE 7 (a) Sea surface slope anomaly at the equator over 10 years estimated from T/P and Jason (end of the time series). The western box is 40W 34W, the eastern box 30W 10W. Although a seasonal cycle dominates, interannual variability is important. Units are mm/degree. (b) Normalized 10-year-long time series of sea surface slope anomaly (top curve) and ERA40 wind stress amplitude at 23W (below). Correlation is 0.67. Year 1997 is anomalous in both time series.

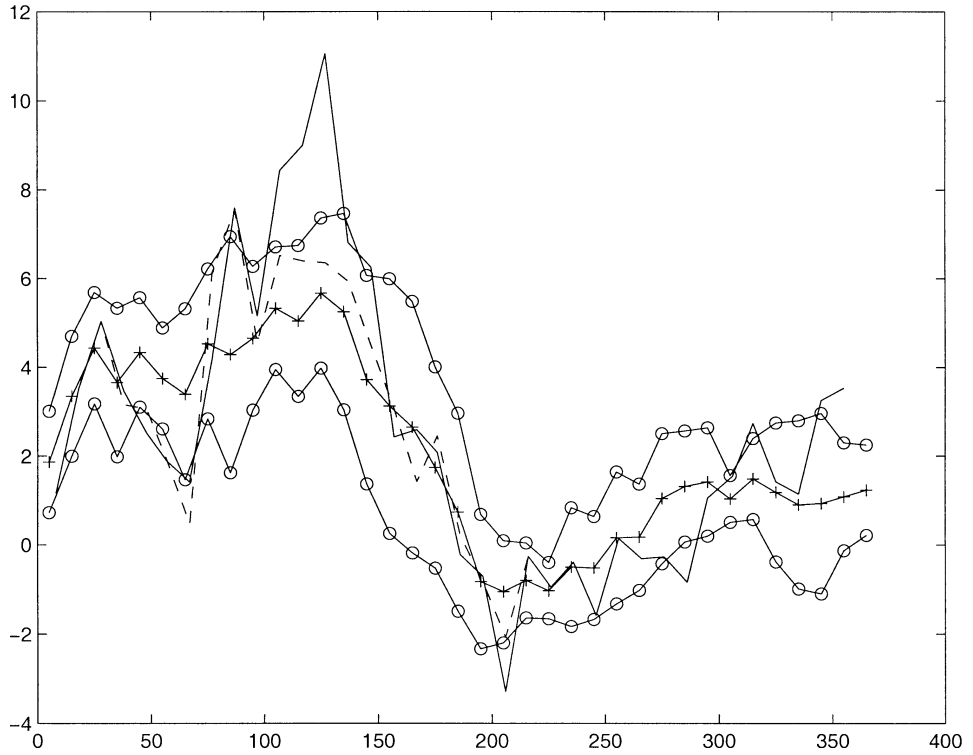

FIGURE 8 SSSA at the equator in 2002, the western box being 40W–34W and the eastern box 30W–10W. Units are mm/degree, time in julian days. Crosses are 10-year mean annual cycle from T/P, and circles one standard deviation above and below this annual mean cycle. Full line is SSSA from Jason cycles 3 to 35; dashed line SSSA from T/P cycles 346 to 363.

Figure 8 shows the equatorial SSSA in 2002 from T/P and Jason compared to the 10-year mean annual variation and its standard deviation. Both Jason-derived and T/P-derived slope anomalies for year 2002 are almost always within one standard deviation of the 10-year mean annual cycle, except in April–May when Jason maximum is higher as already noticed.

Comparison Between Sea Surface Slope from Altimetry and in Situ Current Meter Profiles

As seen in the section on comparisons, T/P and Jason equatorial zonal slope anomaly signals are coherent, and this allows continuing T/P time series with Jason. For year 2002, we have produced two time series of SSSA, one (S1) with T/P data until the end of the commissioning phase (T/P until cycle 364, August 2002), then with Jason data, the other (S2) with T/P data until the beginning of the commissioning phase only (cycle 346, February 2002) then with Jason data (Figure 9). The two time series therefore only differ within the commissioning phase. The slope anomaly is maximum when the winds are the weakest (March, April, and May). There is a strong negative correlation (-0.7) between the wind speed (Figure 5 top) and the slope anomaly (Figure 9). Indeed, most of the year, the easterly trade winds are strong and the absolute slope (unavailable here, as altimetry provided anomaly fields only) is steep and downward towards the east. This slope reduces (Katz et al. 1986) during the

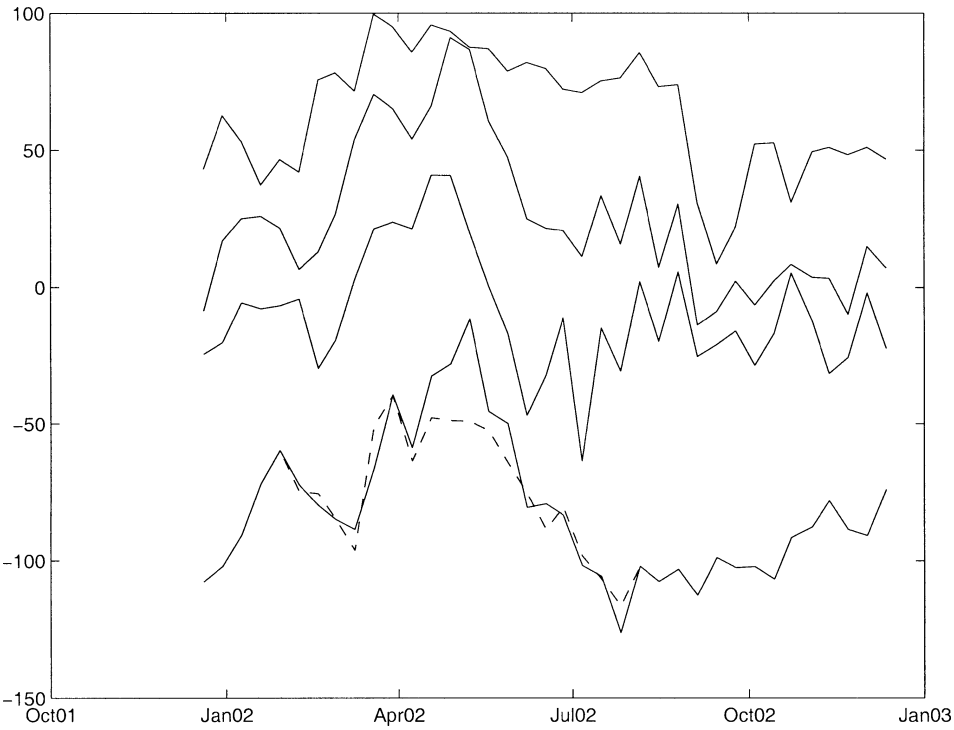

FIGURE 9 Comparison in 2002 between SSSA from altimetry (bottom line) and ADCP zonal velocity respectively at 20, 40, and 60 m depth. (Bottom) dashed line SSSA time series S1 (T/P data in the commissioning phase), full line SSSA time series S2 (Jason data in the commissioning phase). SSSA values are scaled up to be on the same plot as velocities. SSSA values in mm/degree are multiplied by 8 and an offset of 100 is subtracted. Velocity values are in cm/s. The line just above the SSSA represents the velocity at 20 m, above is the velocity at 40 m and the top line is the velocity at 60 m. The 60 m depth is within the EUC and the velocity at 60 m is positive all the time.

shorter period when the wind relaxes (here March to May). Therefore, the slope anomaly with respect to the mean is large during this short period of wind relaxation.

ADCP zonal velocities at 20, 40, and 60 m averaged every 10 days at 23W are also displayed in Figure 9. The 60 m depth is embedded in the EUC and exhibits throughout the year eastward velocities reaching 1 m/s in late March and early April. The 40 m depth level is also mostly in the EUC (eastward velocities except at the beginning and end of the time series). The 20 m depth level is in the near surface westward current except from March to May when the EUC shallows up towards the surface. The strong oscillations associated with TIW, starting in June in the zonal velocity, are visible at 20 and 40 m only.

The SSSA and the zonal velocity are remarkably alike in the upper layer. Correlation coefficients between the zonal velocity at 40 m and SSSA (both S1 and S2) time series exceeds 0.8 (zero phase lag). This depth of 40 m corresponds to the maximum correlation coefficient. This correlation coefficient is slightly smaller above 40 m (for example 0.7 at 20 m and 0.62 at 16 m) and diminishes strongly with depth (it is 0.55 at 60 m, time-lag of about 15 days). All these correlation coefficients are above 0.54 which is the threshold for 95% significance (the degrees of freedom for each time series being computed using the Richman et al. (1977) method). The correlation with time series S2 in which Jason data

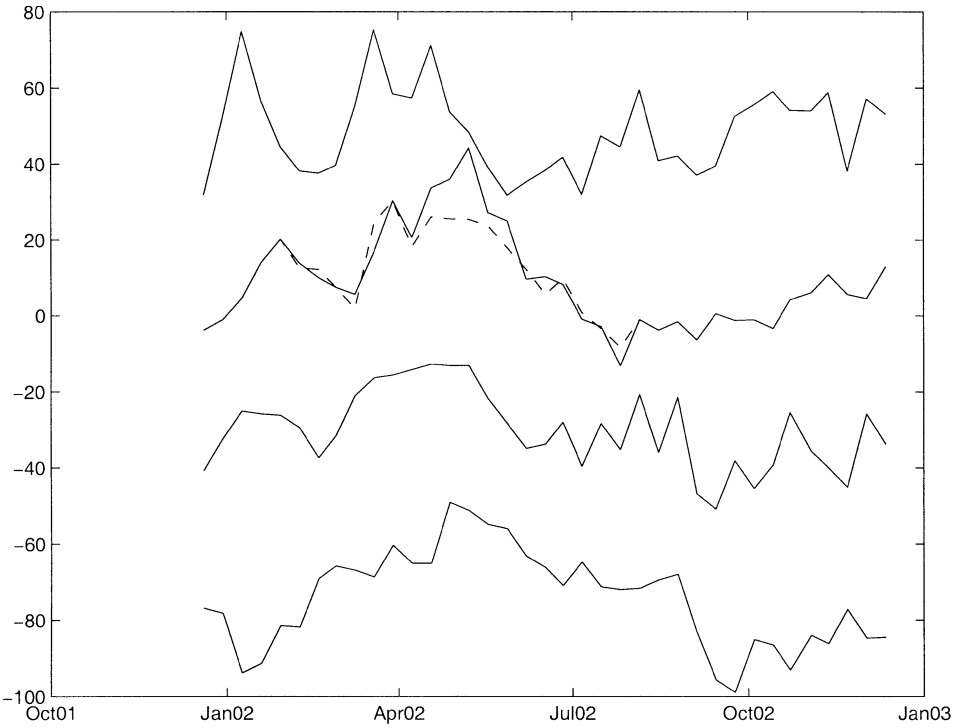

FIGURE 10 Comparison in 2002 between SSSA from altimetry and the depth of the upper limit of the EUC, the depth of the core of the EUC and the EUC transport. Bottom line is the depth of the core of the EUC, the line above the depth of the upper limit of the EUC. Depths are in meters. Line centered on zero is the SSSA time series: dashed line time series S1 (T/P data in the commissioning phase), full line SSSA time series S2 (Jason data in the commissioning phase). SSSA is in mm/degree. The top curve is the integration of the zonal velocity of the EUC along its depth (in m^2/s).

replaces T/P for the commissioning phase is systematically larger by about 0.05 than the correlation with time series S1.

The depths of the upper limit of the EUC and of its core show the seasonal heaving of the EUC (Figure 10): deeper core under stronger winds (and stronger surface westward flow), and shallow core under weaker winds (and weaker or reversed surface flow). The correlations between the SSSA and the upper limit of the EUC, and the depth of the core of the EUC are, respectively, 0.7 (+0.02 for S2) with no time-lag, and 0.55 (+0.03 for S2) with a time-lag of 20 days, both above the 95% significance threshold (0.54). The correlation between the SSSA and the zonal transport of the EUC is poor, about 0.20 (for both S1 and S2) (Figure 10). Again, the correlations are systematically higher with the time series using Jason GDR in the commissioning phase. Depth influence seems to reduce the correlation between "velocity" products and SSSA as the lower correlation is obtained for the depth integrated transport. Time lags as small as those found here are indicative only; the time series have a 10-day sampling. However it may be noted that the lags increase coherently with depth.

Our findings agree with the fact that the surface pressure gradient influence on the zonal velocity diminishes with depth (Wacongne 1989). In the Atlantic, the seasonal changes in the zonal surface pressure gradient are associated with only modest variations in the

depth and speed of the Equatorial Undercurrent. For example, in 1984, the tropical Atlantic experienced a phenomenon similar to El Niño. The zonal pressure gradient along the equator disappeared for a while (Katz et al. 1986); however, the intensity of the EUC was almost unaffected (Weisberg and Colin 1986).

Summary and Discussion

This is a first attempt to compute SSSA from altimetry in the equatorial Atlantic, to examine the sensitivity of this computation, to contrast T/P and Jason in the Atlantic equatorial band over the commissioning phase and compare altimetry derived SSSA to in situ data. The SSSA is computed with an accuracy of about 1 mm/degree, whereas its seasonal variation is on the order of 10 mm/degree. The agreement between Jason and T/P although quite good is not perfect. During three successive cycles the difference between the two slope anomalies is on the order of 3 to 4 mm/degree. The comparison of altimetry-derived SSSA with in situ data is remarkably coherent with our knowledge of the equatorial dynamics in the Atlantic. Comparison with in situ data tends to slightly suggest that the Jason data should be preferred to the T/P data for the three successive cycles which exhibit significant differences. The general agreement proves that Jason ensures a highly reliable continuity of the T/P time series for equatorial slope calculations. A rapid examination of the atmospheric forcing shows that ERA40 wind stress at 23W and the altimetry derived zonal slope anomaly are well correlated and exhibit similar spectral content and similar anomalous years (1997 in particular).

This successful comparison between altimetry-derived equatorial slope anomaly and in situ data in the Atlantic equatorial band opens new areas of investigation. We shall examine precisely the dynamics of the equatorial undercurrent throughout year 2002. We can use temperature and salinity from PIRATA buoys to compute pressure gradient anomaly at depth using the surface value obtained as a reference. We shall also investigate the possibility of computing absolute sea surface slope from altimetry using new products such as recent Mean Sea Surface or satellite marine geoid (GRACE and GOCE missions).

A 10-year-long slope anomaly time series like the one presented in Figure 7a deserves full examination and interpretation. Interannual variability is important and will be carefully examined in relation to the local atmospheric forcing and possible teleconnections. Higher frequencies present in the zonal velocity and in the depth of the EUC could be confronted with altimetry-derived sea surface slopes. A recent article by Kennan and Niiler (2003) shows that, in the tropical Pacific, periods as small as five days can be resolved at the equator if one uses daily equatorial crossings from ERS and T/P. Similar work can be attempted in the Atlantic.

References

Arnault, S., and R. E. Cheney. 1994. Tropical sea level variability from Geosat (1985–1989). *J. Geophys. Res.* 99(C9):18207–18223.

Arnault, S., N. Chouaib, D. Diverrès, S. Jacquin, and O. Coze. 2004. Comparison of TOPEX/Poseidon and JASON altimetry with ARAMIS in situ observations in the tropical Atlantic Ocean. *Mar. Geod.* This issue.

Arnault, S., and E. Kestenare. 2004. Tropical Atlantic surface current variability from 10 years of TOPEX/Poseidon altimetry. *Geophys. Res. Lett.* 31(3): L03308, 10.1029/2003 GL019210.

Fu, L. L., and A. Cazenave, eds. 2001. *Satellite altimetry and earth science,* Int. Geophys. Ser., Vol. 69. San Diego California: Academic Press.

Kartavtseff, A., and C. Provost. 2003. Mouillages courantométriques PIRATA Décembre 2001–Décembre 2002. Rapport interne LODYC n°2003-01.

Katz, E. J. P. Hisard, J. M. Verstraete, and S. L. Garzoli. 1986. Annual change of sea surface slope along the equator of the Atlantic Ocean in 1983 and 1984. *Nature* 222:245–247.

Kennan, S. C., and P. P. Niiler. 2003. Estimating sea surface slope at the equator. *J. Phys. Oceanogr.* 33:2627–2642.

Menard, Y. 1988. Observing the seasonal variability in the tropical Atlantic from altimetry. *J. Geophys. Res.* 93(C11):13967–13978.

Richman, J., C. Wunsch, and N. Hogg. 1977. Space and time scales of mesoscale motion in the western North Atlantic. *Rev. of Geophys. and Space Phys.* 15(4):385–420.

Wacongne, S. 1989. Dynamical regimes of a fully nonlinear stratified model of the Atlantic equatorial undercurrent. *J. of Geophys. Res*. 94(C4):4801–4815.

Weisberg, R. H., and C. Colin. 1986. Equatorial Atlantic ocean temperature and current variations during 1983–1984. *Nature* 322:240–243.

Weisberg, R. H., and T. J. Weingartner. 1988. Instability waves in the equatorial Atlantic Ocean. *J. Phys. Oceanogr.* 18:1641–1657.